

Spectral Corrections Based on Air Mass, Aerosol Optical Depth, and Precipitable Water for CPV Performance Modeling

Marios Theristis, Eduardo F. Fernández, Florencia Almonacid, and Pedro Pérez-Higueras

Abstract—The performance of a concentrating photovoltaic (CPV) system is highly influenced by the spectral variations that are mainly caused by changes in air mass, aerosol optical depth, and precipitable water (PW). Therefore, a spectral correction has to be used in order to correct the incident irradiance and, hence, improve CPV performance modeling. A new procedure that uses a simple set of analytical equations that account for this effect is proposed in this study. A detailed description of how to extract the equations and coefficients of this method is also presented. The experimental validation and the comparative analysis with other methods reported in the literature demonstrated a root-mean-square error (RMSE) of 0.8%, compared with 2.3% of the other methods.

Index Terms—Aerosol optical depth (AOD), air mass (AM), analytical equations, concentrating photovoltaic (CPV), precipitable water (PW), spectral factor (SF).

I. INTRODUCTION

IT is well known that the performance of a photovoltaic (PV) device depends on the distribution of the solar spectrum [1], [2], which, in turn, varies, depending on time and the geographic location. Although cloud cover predominantly affects the PV performance, other parameters such as the air mass (AM), aerosol optical depth (AOD), and precipitable water (PW) also affect the PV performance by modifying the incident spectral irradiance [3].

The effect of the spectral variations is different depending on the PV technology. If such variations are neglected and only the broadband irradiance is used for PV performance modeling,

Manuscript received June 23, 2016; revised August 4, 2016; accepted August 30, 2016. Date of publication September 21, 2016; date of current version October 19, 2016. This work was supported in part by the Spanish Economy Ministry and the European Regional Development Fund/Fondo Europeo de Desarrollo Regional (ENE2013-45242-R) and by the “Plan de Apoyo a la Investigación de la Universidad de Jaén y la Caja Rural de Jaén” (UJA2015/07/01). The work of M. Theristis was supported by the visiting researcher program of the University of Jaén. The work of E. F. Fernández was supported by the Spanish Ministry of Economy and Competitiveness through the Juan de la Cierva 2013 fellowship.

M. Theristis is with the PV Technology Laboratory, FOSS Research Centre for Sustainable Energy, and the Department of Electrical and Computer Engineering, University of Cyprus, Nicosia 1678, Cyprus, and also with the Institute of Mechanical, Process and Energy Engineering, Heriot-Watt University, Edinburgh EH14 4AS, U.K. (e-mail: theristis.marios@ucy.ac.cy).

E. F. Fernández, F. Almonacid, and P. Pérez-Higueras are with the Centro de Estudios Avanzados en Energía y Medio Ambiente, University of Jaén, Jaén 23071, Spain (e-mail: fenandez@ujaen.es; facruz@ujaen.es; pjperes@ujaen.es).

Color versions of one or more of the figures in this paper are available online at <http://ieeexplore.ieee.org>.

Digital Object Identifier 10.1109/JPHOTOV.2016.2606702

then errors of up to 10% can be introduced in extreme conditions [4]. Moreover, concentrating photovoltaic (CPV) systems use multijunction (MJ) solar cells; such cells exhibit a higher spectral sensitivity, compared with single-junction devices, because of the in-series connection of different bandgap solar cells [5]. In this case of MJ solar cells, spectral errors of up to 30% can occur at locations with extreme atmospheric conditions [6]. It is important, therefore, to quantify the spectral influence on the performance of CPV systems.

Several methods have been introduced to account for the spectral sensitivity based on

- 1) direct measurements of the solar spectrum (e.g. using a spectroradiometer [7]);
- 2) spectral indices that characterize the solar spectrum (e.g., average photon energy [8], [9]);
- 3) spectral indices that quantify the effect of solar spectrum on a solar cell (e.g., spectral factor (SF) [10], spectral matching ratio SMR [11], Z parameter [12], etc.).

All these methods, however, require direct measurements by using special devices (e.g., spectroradiometer, isotope sensors) that are not always available. In this work, and for the first time, an analytical procedure is proposed to account for the spectral effect in CPV performance modeling taking into account the AM, AOD at 500 nm, and PW. This procedure can be useful for the CPV performance calculations in locations where atmospheric data are available and bulk spectra simulations [13], [14] are not desirable. For example, the NASA AEROSOL ROBOTIC NETWORK (AERONET) program [15], [16] offers high-quality ground-based observed atmospheric data for over 300 locations worldwide. Therefore, the proposed procedure can estimate the spectral performance of a CPV device without using any measuring or characterization equipment of the solar spectrum.

Analytical equations that evaluate the impact of spectrum on PV devices have been previously suggested in the literature. In particular, the Sandia Array Performance Model (SAPM) applies a fourth-order polynomial correction based on AM; this is known as the AM modifier [17]

$$f_s = f(\text{AM}) = \alpha_0 + \alpha_1 \cdot \text{AM} + \alpha_2 \cdot (\text{AM})^2 + \alpha_3 \cdot (\text{AM})^3 + \alpha_4 \cdot (\text{AM})^4. \quad (1)$$

This method is widely used for the spectral correction in PV performance modeling. It is straightforward to apply since the AM can be calculated from the position of the sun. However, because the spectral irradiance is also affected by AOD and

PW, the fourth-order polynomial fit can be incorrect when these parameters vary during a day [18]. Hence, (1) exhibits a climatic and seasonal dependence. The necessity to improve the prediction accuracy of (1) has also been highlighted by Klise *et al.* [19]. PV_LIB toolbox, a PV performance modeling collaborative formed by the Sandia National Laboratories (SNL) [20], also uses a spectral correction developed by Lee and Panchula of First Solar [21]:

$$f_s = f(\text{AM}, \text{PW}) = \alpha_0 + \alpha_1 \cdot \text{AM} + \alpha_2 \cdot \text{PW} + \alpha_3 \cdot \sqrt{\text{AM}} + \alpha_4 \cdot \sqrt{\text{PW}} + \alpha_5 \cdot \frac{\text{AM}}{\text{PW}} \quad (2)$$

where the “ α ” coefficients in (1) and (2) are determined using multiple linear regression analysis and can be different depending on the PV technology due to their different spectral responses. A method based on artificial neural networks (ANN) that takes into account all the atmospheric parameters has been introduced by Fernández and Almonacid [22]. Although the error was reported to be lower than the AM modifier [root-mean-square error (RMSE) of 2.9% compared with 4.9% of (1)], the ANN method has the clear disadvantage that it requires advanced knowledge of sophisticated computational modeling techniques that are not easily adaptable.

The aim of this paper is to overcome these gaps by introducing a simple set of analytical equations that corrects the solar spectrum and takes into consideration the AM, AOD, and PW. Section II presents the basic theory for the spectral correction, and in Section III, the methodology is explained in detail. Section IV continues with the experimental validation of the proposed procedure, and finally, a comparative study is performed in order to highlight the importance of considering the AM, AOD, and PW.

II. THEORY

In order to determine the impact of the spectral variations on the CPV performance, the short-circuit current density of each i -subcell of an MJ solar cell is required; this is calculated by

$$J_{\text{sc},i} = \text{CR} \cdot \int_{\lambda_{i,\min}}^{\lambda_{i,\max}} \text{SR}_i(\lambda) \cdot \eta_{\text{opt}}(\lambda) \cdot E_b(\lambda) d\lambda \quad (3)$$

where CR is the geometrical concentration ratio (i.e., the ratio of lens' area to cell's area), $\lambda_{i,\min}$ and $\lambda_{i,\max}$ correspond to the wavelength range of the corresponding subcell, SR_i is the spectral response (i.e., the ratio of current generation to the incident power), η_{opt} is the optical efficiency, and $E_b(\lambda)$ is the spectral direct normal irradiance. In the case of a triple-junction (3J) solar cell, i is equal to 1 for top, 2 for middle, and 3 for bottom subcell.

The total current density output is restricted to the minimum due to the in-series connection of the subcells

$$J_{\text{sc,cell}} = \min(J_{\text{sc},i}). \quad (4)$$

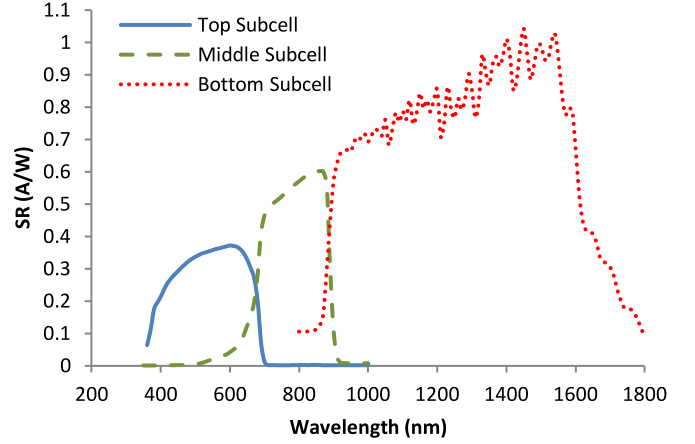


Fig. 1. Spectral response of the Spectrolab C3MJ 3J solar cell at 25 °C.

The spectral correction is evaluated using the SF of each subcell and is expressed as

$$f_{s,i} = \text{SF}_i = \frac{\int E_b(\lambda) \cdot \eta_{\text{opt}}(\lambda) \cdot \text{SR}_i(\lambda) d\lambda}{\int E_b(\lambda) d\lambda} \cdot \frac{\int E_{b,\text{ref}}(\lambda) d\lambda}{\int E_{b,\text{ref}}(\lambda) \cdot \eta_{\text{opt}}(\lambda) \cdot \text{SR}_i(\lambda) d\lambda} = \frac{J_{\text{sc},i}}{E_b} \cdot \frac{E_{b,\text{ref}}}{J_{\text{sc},i}^{\text{ref}}} \quad (5)$$

Having calculated the SF at each subcell, it is possible to calculate the SF of the whole cell by

$$f_s = \text{SF} = \min \left(\text{SF}_i \cdot \frac{J_{\text{sc},i}^{\text{ref}}}{J_{\text{sc,cell}}^{\text{ref}}} \right). \quad (6)$$

This index evaluates the spectral impact on the performance of a high-concentration photovoltaic device as a function of the input spectral irradiance related to the reference spectrum. Hence, a value greater than 1 indicates spectral gains, while a value lower than 1 indicates spectral losses, and a value equal to 1 represents the same spectral conditions to the reference [23].

III. METHODOLOGY

In this study, a set of analytical equations is proposed, in order to calculate the spectral correction of a CPV system as a function of AM, AOD, and PW. To explain the methodology and as an example, a lattice-matched (LM) 3J GaInP/GaInAs/Ge solar cell from Spectrolab was selected; the SR of C3MJ at 25 °C is given in Fig. 1. Any spectral modifications of the incident irradiance due to the concentrating optics were not taken into account (i.e., $\eta_{\text{opt}} = 1$).

In order to characterize the influence of each atmospheric parameter and therefore to extract the analytical equations of each subcell, the Simple Model of the Atmosphere Radiative Transfer of Sunshine, version 2 [24] was used to generate spectra for the following (relatively realistic) ranges:

- 1) $1 \leq \text{AM} \leq 5$, step 0.25 cm;
- 2) $0.05 \leq \text{AOD} \leq 0.6$, step 0.05 cm;

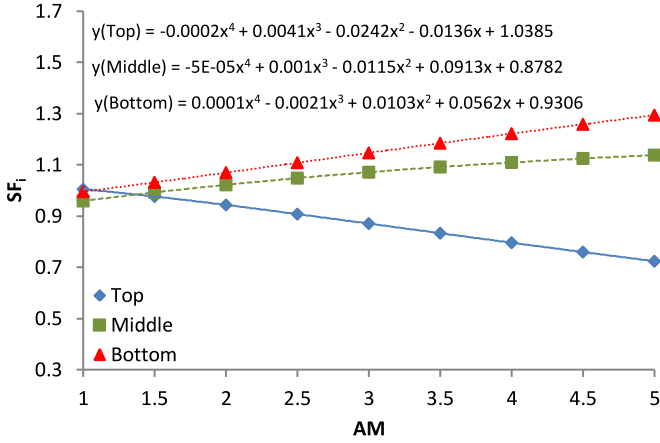


Fig. 2. SF of each subcell against AM for AOD = 0.1 and PW = 1 cm. The fourth-order polynomial fits are also illustrated, where $x = \text{AM}$.

3) $0.25 \leq \text{PW} \leq 4$ cm, step 0.25 cm.

The combinations resulted in 3264 spectra, from where the SF of each subcell and whole 3J solar cell were then calculated using (5) and (6), respectively. The procedure is formulated as follows:

$$f_{s,i} = \text{SF}_i = f(\text{AM}, \text{AOD}, \text{PW})_i \quad (7)$$

and

$$f(\text{AM}, \text{AOD}, \text{PW})_i = f(\text{AM})_i + f(\text{AOD})_i + f(\text{PW})_i \quad (8)$$

where $f(\text{AM})_i$ is (1), and

$$f(\text{AOD})_i = f(\text{AOD coeff.})_i \cdot (\text{AOD} - \text{AOD}_{\text{ref}}) \quad (9)$$

$$f(\text{PW})_i = f(\text{PW coeff.})_i \cdot (\text{PW} - \text{PW}_{\text{ref}}). \quad (10)$$

First, the SF_i is plotted against the AM (Fig. 2 shows an example for AOD = 0.1 and PW = 1 cm). It can be seen that the SF_1 decreases with increasing AM, while SF_2 and SF_3 show an increase for AM values up to 5 [25]. As expected, the fourth-order polynomial suggested in the SAPM [i.e., $f(\text{AM})$ from (1)] fits the SF_i perfectly with a coefficient of determination (R^2) equal to 1.

In order to extract the $f(\text{AOD coeff.})_i$ equations, initially, the SF_i is plotted against the AOD values that are considered. As an example, Fig. 3 illustrates the SF_1 only; the procedure is the same for the other subcells but is not plotted for clarity purposes and space restrictions. The data series are fitted linearly and the coefficients (or slopes) of the fits are extracted and plotted against AM in Fig. 4. The data series in Fig. 4 can be fitted logarithmically for the top and bottom subcells and by using a second-order polynomial for the middle subcell. The R^2 values are 0.99, 1, and 1 for the top, middle, and bottom subcells, respectively.

The same procedure is followed for the $f(\text{PW coeff.})_i$: the SF_i is plotted against the PW for a range of AM values (see Fig. 5 for SF_1), and the slopes of the linear fits are extracted and plotted against the AM in Fig. 6. The top and bottom subcells are

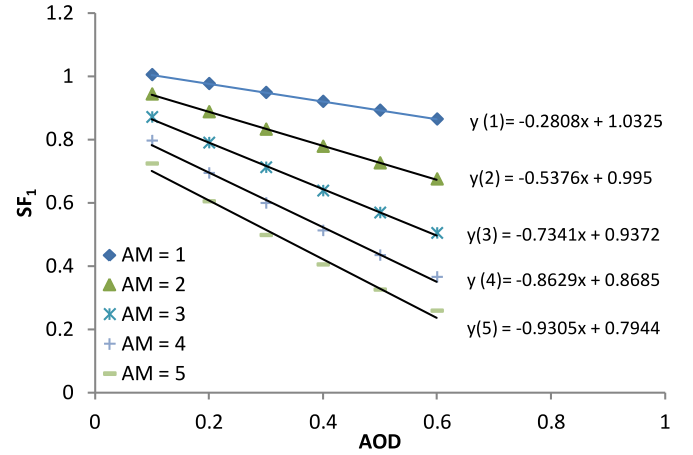


Fig. 3. SF of top subcell against the AOD for a range of AM values. The PW is kept constant at 1 cm. The linear fits are also illustrated, where $x = \text{AOD}$.

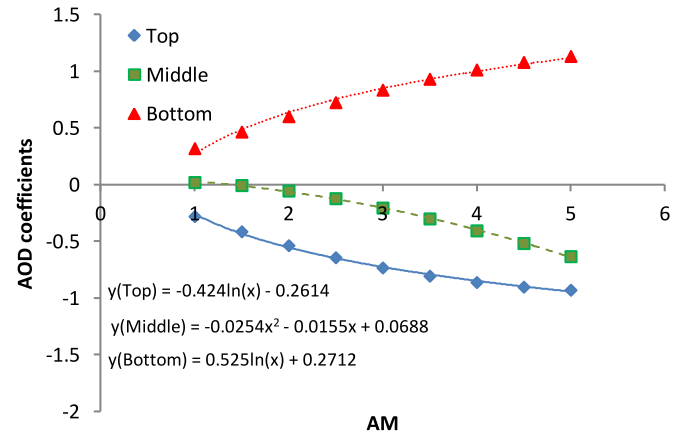


Fig. 4. AOD coefficients as a function of AM for each subcell. The logarithmic (top and bottom subcells) and second-order polynomial (middle subcell) fits are also given, where $x = \text{AM}$.

fitted logarithmically, while the middle subcell is fitted linearly, and the R^2 values are 0.98, 0.97, and 0.99, respectively.

Therefore, the AOD coefficient functions [i.e., (9)] for the top and bottom subcells are calculated by

$$f(\text{AOD coeff.})_{1/3} = \alpha_5 \cdot \ln(\text{AM}) + \alpha_6 \quad (11)$$

while for the middle subcell is

$$f(\text{AOD coeff.})_2 = \alpha_5 \cdot (\text{AM})^2 + \alpha_6 \cdot \text{AM} + \alpha_7. \quad (12)$$

Similarly, from (10), the PW coefficient functions for the top and bottom subcells are estimated using

$$f(\text{PW coeff.})_{1/3} = \alpha_7 \cdot \ln(\text{AM}) + \alpha_8 \quad (13)$$

while for the middle subcell, a linear fit is used as

$$f(\text{PW coeff.})_2 = \alpha_8 \cdot \text{AM} + \alpha_9. \quad (14)$$

Once the equations are extracted, the α -coefficients are estimated by performing a multiple linear regression analysis on outdoor measured data. For guidance, the equations are also given in Table I.

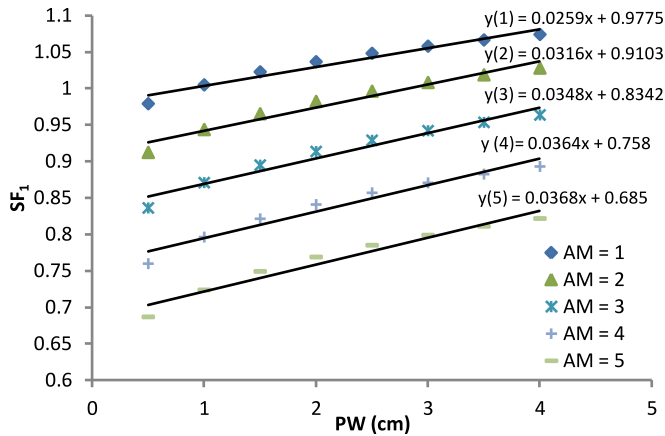


Fig. 5. SF of top subcell against the PW for a range of AM values. The AOD is kept constant at 0.1. The linear fits are also illustrated, where $x = PW$.

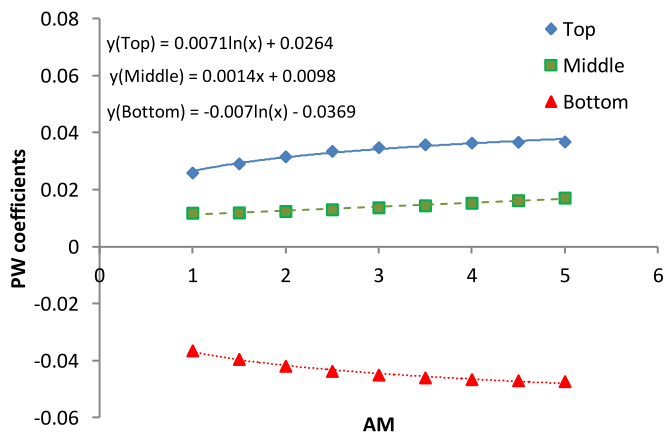


Fig. 6. PW coefficients as a function of AM. The logarithmic (top and bottom subcells) and linear (middle subcell) fits are also given, where $x = AM$.

TABLE I
PROPOSED SPECTRAL CORRECTIONS AT EACH SUBCELL

Correction for:	AM	AOD coeff.	PW coeff.
SF ₁	$ax^4 + bx^3 + cx^2 + dx + e$	$a \ln(x) + b$	$a \ln(x) + b$
SF ₂	$ax^4 + bx^3 + cx^2 + dx + e$	$ax^2 + bx + c$	$ax + b$
SF ₃	$ax^4 + bx^3 + cx^2 + dx + e$	$a \ln(x) + b$	$a \ln(x) + b$

where $x = AM$.

IV. ANALYSIS OF THE PROPOSED PROCEDURES

A. Experimental Validation

A 3-mo experiment was conducted at the Centro de Estudios Avanzados en Energía y Medio Ambiente (CEAEMA), University of Jaén, Spain (37.2796° N, 3.2812° W) from March until May 2016.

A solar spectral irradiance meter (SolarSIM-D2) from Spectrafy Inc. [26], [27] was used to measure the spectral direct normal irradiance (280–4000 nm), AOD at 500 nm, and PW and, hence, to validate the analytical equations described earlier. The high accuracy of such devices was reported by the manufacturing company through tests conducted in the National Renewable

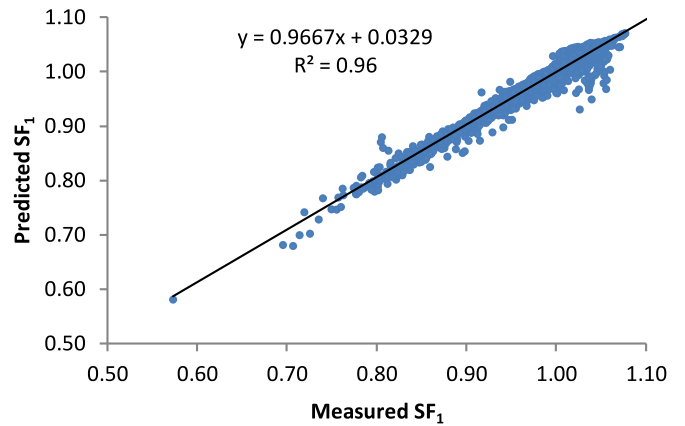


Fig. 7. Predicted SF₁ using the proposed method against the measured SF₁ for $R^2 = 0.96$.

Energy Laboratory [27]. The AM was calculated as a function of the sun's zenith angle (z) [28]

$$AM = \frac{1}{\cos z + 0.50572 \cdot (96.07995 - z)^{-1.6364}}. \quad (15)$$

The SolarSIM-D2 was mounted on a BSQ Solar two-axis solar tracker, located on the rooftop of the building where the CEAEMA is based. Irradiance and atmospheric data were recorded every 5 min through Ethernet connection.

In order to avoid the influence of moving clouds on the measurements and to ensure realistic values for the specific location, the outdoor data were filtered for

- 1) 5-min DNI variation < 5%;
- 2) $0.01 < AOD < 0.5$.

The second filter is applied to remove any physically false values (in this case, they were less than 1% of the dataset) for the particular location (Jaén, Spain) during the time of measurements; the procedure is expected to be valid for locations where greater AOD values occur. This filter can also be partially confirmed by comparing a recent study conducted by Ruiz-Arias *et al.* [29], where a mean AOD (at 1020 nm) of 0.09 was reported for an AERONET station in Granada (approximately 65 km away from the CEAEMA). It is also worth mentioning that there was an attempt made to use straightforward filtering criteria in order to reduce the number of filters, as well as avoid the use of complex ones (that, in turn, may require special measuring equipment).

The measured spectra were then used to calculate the SF_{*i*} in order to compare with the ones estimated using the analytical equations. The comparisons between the SF_{*i*} predicted by the proposed procedure against the measured ones are illustrated in Figs. 7–9 for SF₁, SF₂, and SF₃, respectively, for a total of 4014 data points. Very good agreement between predicted and measured SF_{*i*} has been achieved for all subcells with R^2 values of the linear fits being 0.96, 0.99, and 0.95 for the top, middle, and bottom subcell, respectively.

Using (6), the whole 3J solar cell's SF was calculated for the proposed procedure and measured data; the comparison is also illustrated in Fig. 10 showing a coefficient of determination equal to 0.97.

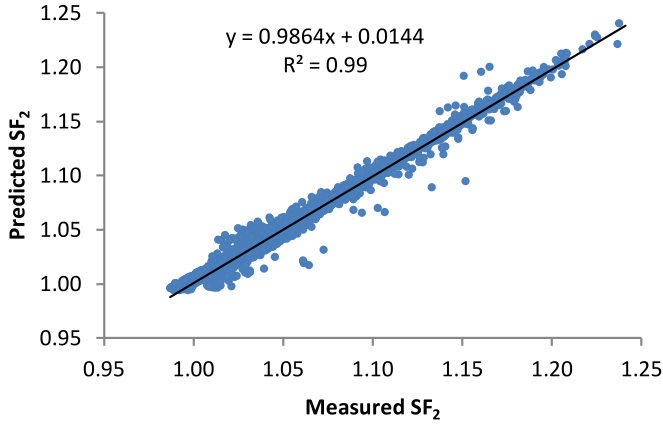


Fig. 8. Predicted SF₂ using the proposed method against the measured SF₂ for $R^2 = 0.99$.

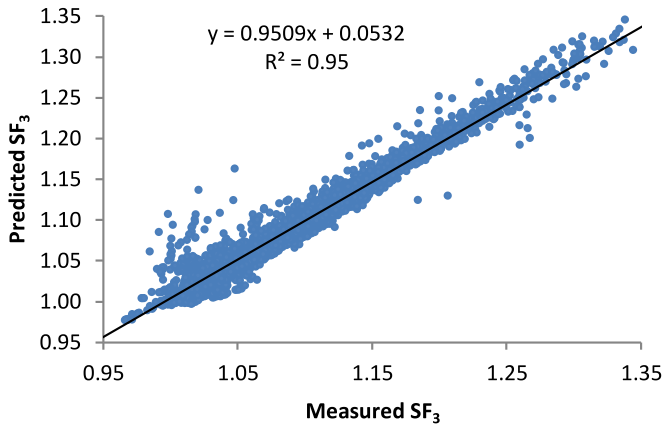


Fig. 9. Predicted SF₃ using the proposed method against the measured SF₃ for $R^2 = 0.95$.

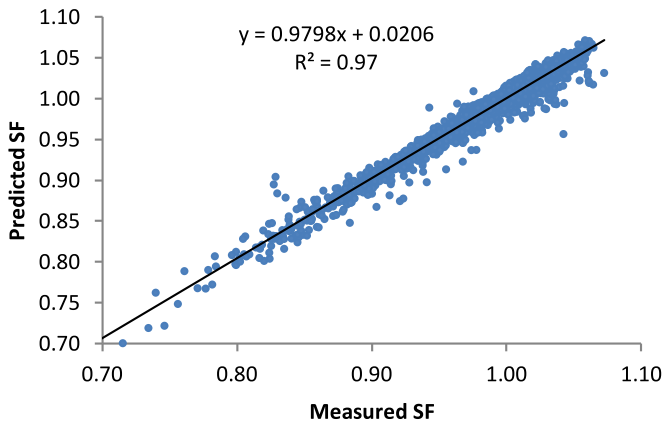


Fig. 10. Predicted SF using the proposed method against the measured SF for $R^2 = 0.97$.

B. Comparative Analysis

In order to examine the accuracy of the proposed methods against (1) of Sandia Labs and (2) of First Solar, a comparative analysis has also been performed. In order to reiterate, (1) takes into consideration AM only, while (2) accounts for AM and PW.

TABLE II
REGRESSION COEFFICIENTS FOR ALL METHODS

coeff.	Proposed procedure			Sandia Labs	First Solar
	SF ₁	SF ₂	SF ₃	SF _{SAPM}	SF _{FS}
α_0	1.0538	0.9392	0.9717	0.8245	0.5998
α_1	-0.0003	0.0001	0.0003	-0.0019	-0.1793
α_2	0.0054	-0.0020	-0.0040	0.0303	-0.1000
α_3	-0.0311	0.0044	0.0193	-0.1667	0.3768
α_4	0.0125	0.0607	0.0329	0.3210	0.2970
α_5	-0.7652	-0.0393	0.8786		0.0163
α_6	-0.1791	0.2020	0.2407		
α_7	0.0234	-0.1059	-0.0337		
α_8	0.0288	0.0014	-0.0446		
α_9		0.0107			

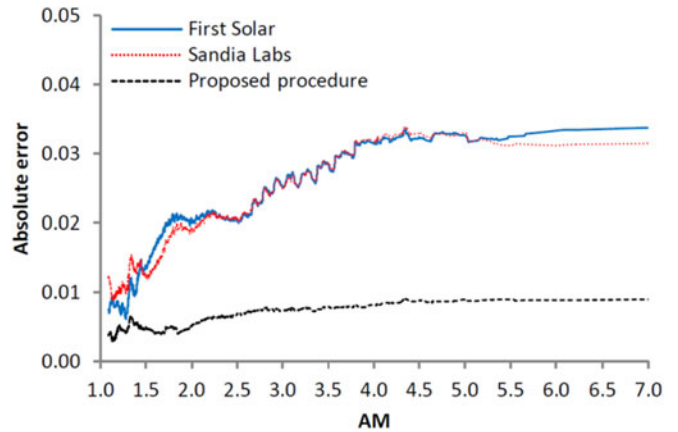


Fig. 11. AE between measured SF and the SF calculated by each of the three methods that are compared against the AM.

The regression coefficients for all methods are listed in Table II. As previously commented, and in order to validate and compare the procedure in a straightforward manner, these coefficients do not take into account any spectral modifications caused by the concentrating optics. It should be mentioned, however, that the procedure and equations would remain the same, since the trends of SF_i over AM, AOD, and PW are not affected by the spectral optical efficiency [23].

The absolute error (AE) of each method against the measured SF have been plotted for all AM, AOD, and PW values in Figs. 11–13, respectively. In Fig. 11, the trend shows that the proposed procedure remains relatively constant with increasing AM, while the Sandia Labs and First Solar methods exhibit a significant increase.

Similar to Fig. 11, the proposed procedure remains relatively constant at all AOD values, while the Sandia Labs and First Solar methods increase with increasing AOD (see Fig. 12). It can also be noticed that the lowest AE for Sandia Labs and First Solar methods are exhibited at low AOD values (near reference conditions AOD = 0.084).

In Fig. 13, the proposed procedure is relatively constant, in a similar way as in Figs. 11 and 12. Despite the spikes, it is clear that the AE is higher for the Sandia Labs and First solar methods, with First Solar exhibiting lower errors for PW > 2.25 cm.

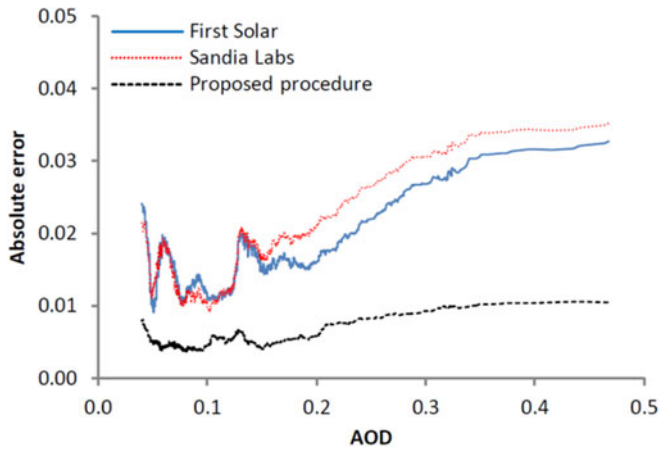


Fig. 12. AE between measured SF and the SF calculated by each of the three methods that are compared against the AOD.

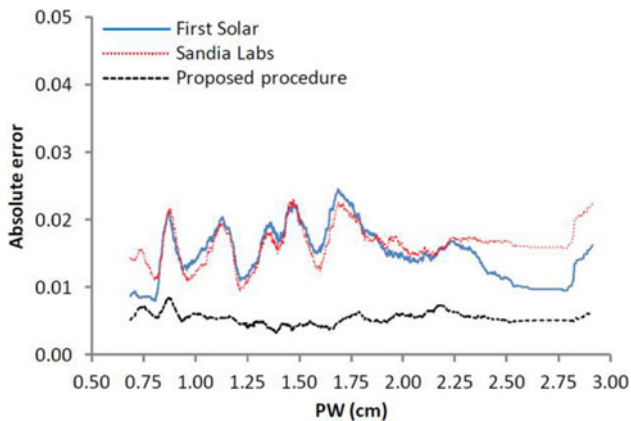


Fig. 13. AE between measured SF and the SF calculated by each of the three methods that are compared against the PW.

TABLE III
ERRORS AND COMPARISON WITH OTHER METHODS

Method	RMSE	MBE
Proposed	0.8%	0.04%
First Solar	2.3%	0.06%
Sandia Labs	2.3%	0.07%

It is important to highlight here the trends of the Sandia Labs and First Solar methods that use (1) and (2), respectively, as compared with the proposed one of this study. The increasing AE with increasing AOD could act as a justification of why the fourth-order polynomial correction (1) usually presents a high climatic and location dependence (see also the Introduction). Especially, in locations with high AOD (e.g., Kuwait and Kanpur [30]) and PW (e.g., Tenosique and Kaashidhoo [30]), the error in the performance estimation could be significantly higher if AOD and PW are not incorporated in the spectral correction of each subcell and, hence, the whole cell.

In Table III, the RMSE and mean bias error (MBE) are given for all methods. With regard to RMSE, the proposed procedure presents the lowest error of 0.8%, while the First Solar and

Sandia Labs methods show an error of 2.3%. The MBE is close to zero in all cases, which shows that the procedures neither overestimate nor underestimate the SF.

Overall, the proposed procedure exhibited a better performance compared with the others reported in the literature. Considering that the comparison was conducted in Jaén, Spain which is generally characterized by low AOD and PW values, it is expected that the proposed method would outperform the other methods in a greater extent in locations with extreme atmospheric characteristics. This should be the topic of future work.

V. CONCLUSION

A new procedure has been proposed for the spectral correction of MJ solar cells based on AM, AOD, and PW for CPV performance modeling. The advantage of the method is that it accounts for the main parameters that change the spectrum, and therefore, the climatic and location dependences of the other methods reported in literature can be eliminated.

The procedure to obtain the analytical equations was explained step by step and the validation was performed using outdoor measurements from Jaén, Spain. The validation of predicted SF showed a good agreement of the method with a determination coefficient of 0.97 for an LM 3J solar cell.

A comparative analysis has also been conducted in order to observe how the method performs against others that have been reported in the literature, as well as to highlight the importance of developing a spectral correction based on the main parameters that affect the spectrum in CPV. The comparison showed that the proposed method yields lower errors with a minimum RMSE of 0.8%. In addition, the AE of the Sandia Labs and First Solar methods exhibited a growing trend, especially with increasing AM and AOD. Since Jaén is a location with relatively low average AOD and PW values, it is expected that the significance of the proposed procedure could be demonstrated in a location with extreme atmospheric conditions.

Future work will propose analytical equations and the corresponding coefficients for the spectral correction of multiple PV technologies and also CPV modules including the spectral characteristics of the optical components. In addition, locations with extreme atmospheric characteristics will be evaluated, and the importance of the procedure will be highlighted.

REFERENCES

- [1] S. Nann and K. Emery, "Spectral effects on PV-device rating," *Sol. Energy Mater. Sol. Cells*, vol. 27, pp. 189–216, Aug. 1992.
- [2] D. L. King, J. A. Kratochvil, and W. E. Boyson, "Measuring solar spectral and angle-of-incidence effects on photovoltaic modules and solar irradiance sensors," in *Proc. 26th IEEE Conf. Rec. Photovoltaic Spec. Conf.*, 1997, pp. 1113–1116.
- [3] B. Marion, "Influence of atmospheric variations on photovoltaic performance and modeling their effects for days with clear skies," in *Proc. 38th IEEE Photovoltaic Spec. Conf.*, 2012, pp. 3402–3407.
- [4] R. Gottschalg, T. R. Betts, D. G. Infield, and M. J. Kearney, "The effect of spectral variations on the performance parameters of single and double junction amorphous silicon solar cells," *Sol. Energy Mater. Sol. Cells*, vol. 85, pp. 415–428, 2005.
- [5] P. Faine, S. R. Kurtz, C. Riordan, and J. M. Olson, "The influence of spectral solar irradiance variations on the performance of selected single-junction and multijunction solar-cells," *Sol. Cells*, vol. 31, pp. 259–278, Jun. 1991.

- [6] E. F. Fernández, A. Soria-Moya, F. Almonacid, and J. Aguilera, "Comparative assessment of the spectral impact on the energy yield of high concentrator and conventional photovoltaic technology," *Sol. Energy Mater. Sol. Cells*, vol. 147, pp. 185–197, 2016.
- [7] M. Norton *et al.*, "Analysis of the output of two isotype cell sets compared to a precision spectroradiometer," in *Proc. AIP Conf.*, 2015, vol. 1679, p. 050008.
- [8] C. Jardine, T. R. Betts, R. Gottschalg, D. G. Infield, and K. Lane, "Influence of spectral effects on the performance of multijunction amorphous silicon cells," in *Proc. 17th Eur. Photovoltaic Sol. Energy Conf.*, 2002.
- [9] S. R. Williams *et al.*, "Modelling long-term module performance based on realistic reporting conditions with consideration to spectral effects," in *Proc. 3rd World Conf. Photovoltaic Energy Convers.*, 2003, vol. 2, pp. 1908–1911.
- [10] E. F. Fernández, F. Almonacid, A. Soria-Moya, and J. Terrados, "Experimental analysis of the spectral factor for quantifying the spectral influence on concentrator photovoltaic systems under real operating conditions," *Energy*, vol. 90, pp. 1878–1886, 2015.
- [11] C. Domínguez, I. Antón, G. Sala, and S. Askins, "Current-matching estimation for multijunction cells within a CPV module by means of component cells," *Prog. Photovoltaics, Res. Appl.*, vol. 21, pp. 1478–1488, 2013.
- [12] M. Meusel, R. Adelhelm, F. Dimroth, A. W. Bett, and W. Warta, "Spectral mismatch correction and spectrometric characterization of monolithic III-V multi-junction solar cells," *Prog. Photovoltaics, Res. Appl.*, vol. 10, pp. 243–255, Jun. 2002.
- [13] C. Stark and M. Theristis, "The impact of atmospheric parameters on the spectral performance of multiple photovoltaic technologies," in *Proc. 42nd IEEE Photovoltaic Spec. Conf.*, 2015, pp. 1–5.
- [14] M. Theristis, C. Stark, and T. S. O'Donovan, "Determination of the cooling requirements for single cell photovoltaic receivers under variable atmospheric parameters," in *Proc. 42nd IEEE Photovoltaic Spec. Conf.*, 2015, pp. 1–5.
- [15] *Aerosol Robotic Network*, 2015. [Online]. Available: <http://aeronet.gsfc.nasa.gov/>
- [16] B. N. Holben *et al.*, "AERONET—A federated instrument network and data archive for aerosol characterization," *Remote Sens. Environ.*, vol. 66, pp. 1–16, 1998.
- [17] D. L. King, W. E. Boyson, and J. A. Kratochvil, "Photovoltaic array performance model," Sandia Labs, Albuquerque, NM, USA, *Rep. SAND 2004-3535*, 2004.
- [18] C. R. Osterwald, K. A. Emery, and M. Muller, "Photovoltaic module calibration value versus optical air mass: The air mass function," *Prog. Photovoltaics, Res. Appl.*, vol. 22, pp. 560–573, 2014.
- [19] K. A. Klise, C. W. Hansen, and J. S. Stein, "Dependence on geographic location of air mass modifiers for photovoltaic module performance models," in *Proc. 42nd IEEE Photovoltaic Spec. Conf.*, 2015, pp. 1–5.
- [20] J. S. Stein, "The photovoltaic performance modeling collaborative (PVMC)," in *Proc. 38th IEEE Photovoltaic Spec. Conf.*, 2012, pp. 3048–3052.
- [21] M. Lee and A. Panchula, "Combined air mass and precipitable water spectral correction for PV modelling," in *Proc. 4th PV Perform. Model. Monit. Workshop*, Cologne, Germany, 2015.
- [22] E. F. Fernández and F. Almonacid, "Spectrally corrected direct normal irradiance based on artificial neural networks for high concentrator photovoltaic applications," *Energy*, vol. 74, pp. 941–949, 2014.
- [23] E. F. Fernández, F. Almonacid, J. A. Ruiz-Arias, and A. Soria-Moya, "Analysis of the spectral variations on the performance of high concentrator photovoltaic modules operating under different real climate conditions," *Sol. Energy Mater. Sol. Cells*, vol. 127, pp. 179–187, 2014.
- [24] C. A. Gueymard, "Simple Model of the Atmospheric Radiative Transfer of Sunshine, Version 2 (SMARTS2): Algorithms Description and Performance Assessment. Cocoa, FL, USA: Florida Sol. Energy Center, 1995.
- [25] M. Theristis, E. F. Fernández, C. Stark, and T. S. O'Donovan, "A theoretical analysis of the impact of atmospheric parameters on the spectral, electrical and thermal performance of a concentrating III-V triple-junction solar cell," *Energy Convers. Manag.*, vol. 117, pp. 218–227, 2016.
- [26] V. Tatsiankou, K. Hinzer, H. Schriemer, J. Haysom, and R. Beal, "A novel instrument for cost-effective and reliable measurement of solar spectral irradiance," in *Proc. 42nd IEEE Photovoltaic Spec. Conf.*, New Orleans, LA, USA, 2015, pp. 1–4.
- [27] V. Tatsiankou *et al.*, "Design principles and field performance of a solar spectral irradiance meter," *Sol. Energy*, vol. 133, pp. 94–102, 2016.
- [28] F. Kasten and A. T. Young, "Revised optical air mass tables and approximation formula," *Appl. Opt.*, vol. 28, pp. 4735–4738, Nov. 15, 1989.
- [29] J. A. Ruiz-Arias, C. A. Gueymard, S. Quesada-Ruiz, F. J. Santos-Alamillos, and D. Pozo-Vázquez, "Bias induced by the AOD representation time scale in long-term solar radiation calculations. Part 1: Sensitivity of the AOD distribution to the representation time scale," *Sol. Energy*, Jun. 21, 2016, Available: <http://dx.doi.org/10.1016/j.solener.2016.06.026>.
- [30] C. A. Gueymard, "Daily spectral effects on concentrating PV solar cells as affected by realistic aerosol optical depth and other atmospheric conditions," *Proc. SPIE*, vol. 7410, 2009, Art. no. 741007.

Authors' photographs and biographies not available at the time of publication.